Molecular Crystals and Liquid Crystals Science and Technology. Section A. Molecular Crystals and Liquid Crystals

Publication details, including instructions for authors and subscription information:
http://www.tandfonline.com/loi/gmcl19

A Novel Polymer — Liquid Crystal System for Display Applications

S. P. Palto [a], L. M. Blinov [a], V. F. Petrov [b], S. V. Jablonsky [a], S. G. Yudin [a], H. Okamoto [b] & S. Takenaka [b]

[a] Institute of Crystallography, Russian Academy of Sciences, Leninsky pr. 59, Moscow, 117333, Russia

[b] Department of Advanced Materials Science and Engineering, Faculty of Engineering, Yamaguchi University, Tokiwadai 2557, Ube, Yamaguchi, 755, Japan

Version of record first published: 24 Sep 2006

To cite this article: S. P. Palto, L. M. Blinov, V. F. Petrov, S. V. Jablonsky, S. G. Yudin, H. Okamoto & S. Takenaka (1999): A Novel Polymer — Liquid Crystal System for Display Applications, Molecular Crystals and Liquid Crystals Science and Technology. Section A. Molecular Crystals and Liquid Crystals, 326:1, 259-278

To link to this article: http://dx.doi.org/10.1080/10587259908025419

Mol. Cryst. Liq. Cryst., Vol. 326, pp. 259–278
Reprints available directly from the publisher
Photocopying permitted by license only

A Novel Polymer – Liquid Crystal System for Display Applications

S. P. PALTO[a], L. M. BLINOV[a], V. F. PETROV[b,*], S. V. JABLONSKY[a], S. G. YUDIN[a], H. OKAMOTO[b] and S. TAKENAKA[b]

[a] *Institute of Crystallography, Russian Academy of Sciences, Leninsky pr. 59, Moscow, 117333, Russia;*
[b] *Department of Advanced Materials Science and Engineering, Faculty of Engineering, Yamaguchi University, Tokiwadai 2557, Ube, Yamaguchi 755, Japan*

(Received 30 June 1998; In final form 13 October 1998)

We present a novel polymer–liquid crystal system based on the monolayers of polymer microballs. These monolayers were prepared on the water surface and then transferred onto the solid substrates by the Langmuir–Blodgett technique. The results of the optical and diffraction studies of prepared films of polymer microballs demonstrate that the microballs are well-packed in the monolayers. We found that polymer microball monolayers can be used with the liquid crystals in a novel polymer–liquid crystal system which is suitable for display applications.

Keywords: Polymer microballs; Langmuir–Blodgett technique; display applications

1. INTRODUCTION

In the past decade, a new application of the liquid crystals has been gaining considerable attention, *i.e.*, the encapsulation of microdroplets of the nematic liquid crystals in solid polymer matrices [1–3]. These polymer–liquid crystal systems are commonly called PDLCs (polymer dispersed liquid crystals) [1] and NCAP (nematic curvilinear aligned phase) [2] and utilize the effect of light-scattering at boundary layers.

Here, we present a novel polymer–liquid crystal system based on the monolayer of polymer microballs. We applied the Langmuir–Blodgett (LB)

*Corresponding author.

technique for the preparation of monolayers of macroscopic objects such as polymer microballs. So far the method developed by I. Langmuir and K. Blodgett [4–5] was used to prepare mono- and multilayers of organic molecules. The essence of the method is that amphiphilic molecules on the water surface can be arranged as a monomolecular layer, which can be transferred onto a solid substrate. Ultrathin molecular films prepared by this method are known as Langmuir–Blodgett films. Despite the fact that it is almost obvious that not only molecules but even macroscopic objects placed on the water surface can be somehow arranged as a monolayer, there is no mention in the literature on study of this phenomenon.

In this work, we studied how polymer microballs ($d = 4.5\,\mu m$) placed on the water surface can be organized as a dense monolayer. We also successfully applied different techniques to transfer the microball monolayers onto the solid substrates.

We found that microball monolayers prepared by the LB method are of rather good quality and can be used for liquid crystal display applications. Moreover, we believe that the results obtained in this work have also a fundamental significance for the LB method in its traditional application demonstrating that amphiphility is not always necessary for preparing well-ordered films.

2. PREPARATION OF MICROBALL MONOLAYERS

2.1. Equipment and Software

Herein we describe the different kinds of equipment used for the investigation of microball monolayers (MBM) on a water surface and transferring MBM onto solid substrates.

Figure 1 shows the experimental set-up allowing a direct observation of the MBM both on a water surface (spreading of microballs on the water surface; formation of a dense monolayer of microballs by compression produced by the moving barrier) and on a substrate. The set-up is based on an optical microscope (3) equipped with a video camera (1), TV monitor (2), a video recorder (7) and a mini trough (6). The trough is made of teflon and has a glass bottom to allow observations by microscope. The working area of the trough is changed by the moving barrier (5).

The equipment used for the preparation of both Langmuir–Blodgett films and MBM is shown in Figure 2. This set-up was designed for the preparation of polar and heterogeneous LB films [6] and includes the following main parts:

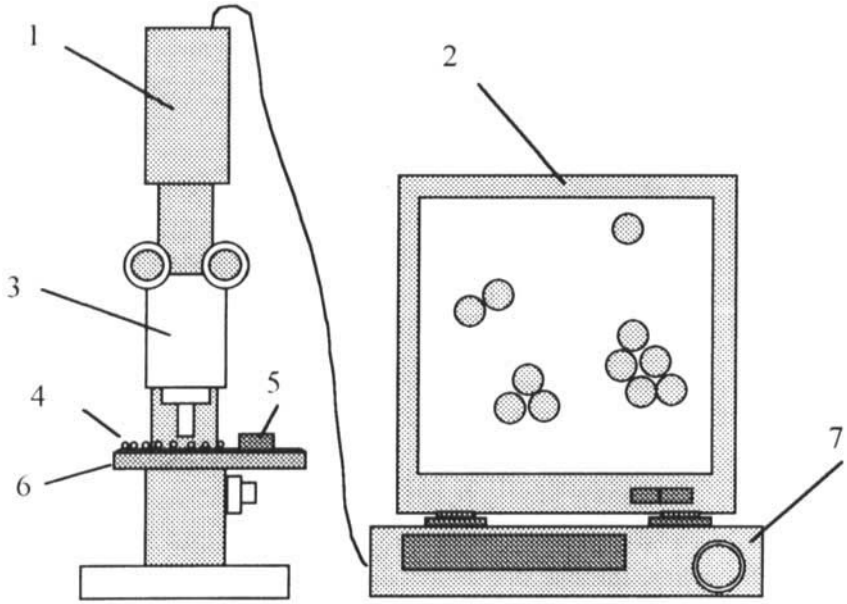

FIGURE 1 Experimental set-up for the investigation of MBM on a water surface. 1) video-camera; 2) TV monitor; 3) microscope; 4) microballs on the water surface; 5) moving barrier; 6) teflon trough; 7) video recorder.

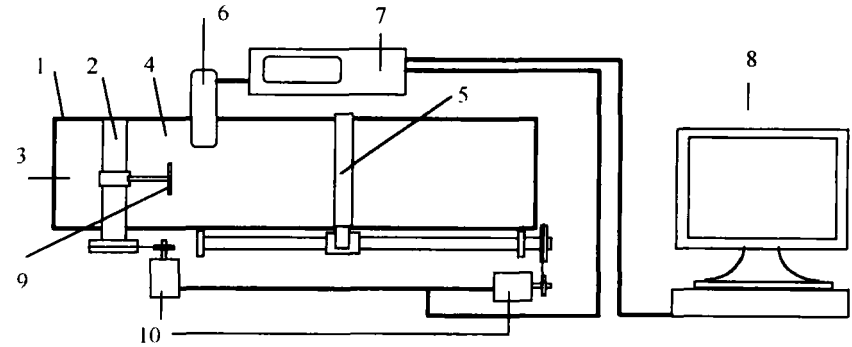

FIGURE 2 Experimental set-up for the preparation of MBM and LB films (top view). 1) trough; 2) barrier mechanism; 3) buffer zone; 4) working area; 5) moving barrier; 6) surface tension meter; 7) microprocessor control and measuring system; 8) computer; 9) substrate holder; 10) motors.

The trough (1) is filled up with pure distilled water. The water surface is divided into two parts by a barrier mechanism (2). The part of the smaller area (3) is called the buffer zone. The second part (4) is called the working region. The area of this region is changed by a moving barrier (5). The

surface of the working region is occupied by the microballs. Thus, the decrease of the working area by moving the barrier results in a decrease of the average distance between the microballs. The extent of the ball packing (monolayer density) is measured with help of a tension meter (6). The equipment is controlled by the microprocessor system (7) allowing communication with an external computer (8). The substrate is fixed to the holder (9) and can be rotated with a defined speed in any direction. We developed special software for the investigation of the behaviour of MBM on the water surface and transferring it onto a solid substrate. The basic possibilities of the software are as follows:

1) measurements of π -A curves (surface pressure π *versus* average area A occupied by a microball);
2) automatic support of a given surface pressure;
3) automatic transfer of the MBM onto a substrate.

The MBM was transferred onto the substrate as a result of the rotation of the substrate first through the buffer zone (3) and finally through the compressed monolayer in the working area (4).

2.2. Polymer Microballs on the Water Surface

The microballs are made of a polymer material with a density higher than that of the pure water. So, at least two questions arise: i) why the microballs can be floating on the water surface and ii) how the microballs can be introduced onto the water surface.

It is obvious that those balls, which are in the bulk of the water, will drop to the bottom. Their movement is influenced only by two external forces such as gravity F_G and Archimed force F_A. Since the density of the polymer ρ is higher than that of the water, the microballs will fall to the bottom with a speed ν defined by the difference between these forces and the viscosity η of the water:

$$\nu \propto \frac{F_G - F_A}{6\pi r\eta} = \frac{2r^2\Delta\rho g}{9\eta} \tag{1}$$

Taking the microball radius $r = 2.25\,\mu m$, the difference in the density between the water and the polymer $\Delta\rho = 100\,kg\ m^{-3}$, the water viscosity $\eta = 0.9\ 10^{-2}$ Poise, we evaluate the falling speed of $1.3\ 10^{-7}\ ms^{-1}$. Thus, the speed is so small that it takes more than one day for microballs to fall onto the bottom.

The situation on the water surface is different. The polymer microballs turned out to be hydrophobic, and due to the surface tension an additional force, which pushes the microballs out, arises. This makes the microballs placed on the water surface float. At first glance, due to the low descent speed of the balls, the water itself can be a good candidate to prepare the weighted mixture of the microballs in the water bulk and to use this mixture for putting the microballs onto the water surface. Experimentally, we found that, in principle, the method works.

Nevertheless, we also found that putting the microballs onto the water surface from the other water mixture of the microballs leads to a significant loss of the microballs. The majority of the microballs goes into the bulk but not onto the surface. Thus, to accumulate a sufficient quantity of the microballs on the surface, one needs to spread too much of the mixture. It results in another problem related to the increase of impurities on the water surface that prevents the formation of the homogeneous microball monolayer. The best candidate we found to prepare the weighted mixture of the microballs was ethanol.

The viscosity and density of the alcohol are less in comparison with those of the water. Nevertheless, the falling speed is still small enough to allow working with a weighted mixture of the microballs in the alcohol. As we observed, due to the lower density of the alcohol, the majority of the microballs remains on the water surface after spreading the alcohol mixture.

We used the mixture of 100 mg of microballs per 40 cm^3 of ethanol. Figure 3 demonstrates the microball monolayer on the water surface. The microballs are still macroscopic objects. Their movement is not influenced significantly by thermal fluctuations, while Van-der-Waals forces are still important. It results in the formation of microball domains. The increase of the mixture amount we spread gives the proper increase of the monolayer density, Figure 3(b). The same result can be obtained by compressing the microballs on the water surface.

A quite important problem in the formation of the microball monolayer on the water surface is related to the measurements of its density. We would like to point out one method traditionally used in the LB technique and associated with the measurements of the surface tension. We believe that there is a quite different physical mechanism of the microball's influence on the surface tension. In the case of the Langmuir monolayer, the change of the surface tension is attributed to the lateral pressure produced by packing molecules on the water surface. As we already mentioned, the kinetic factor is negligible for macroscopic objects such as the microballs. Thus the microballs do not produce any lateral pressure. For this reason it seems that

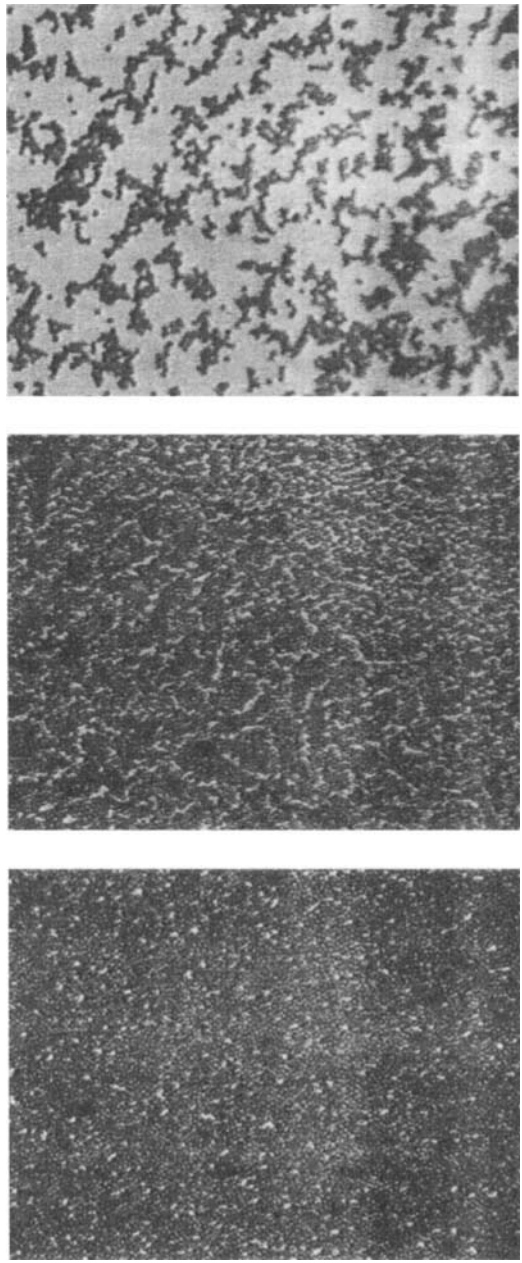

FIGURE 3 Photographs of microball monolayer on the water surface at low (a) and higher densities (b), (c) magnified in 100 times.

a change of the surface density of the microballs should not influence the measurements of the surface tension of the water. The latter is not true. To understand the problem one needs to be reminded that the surface tension is a result of the different molecular orientation of the molecules in the bulk and on the interface. Of course, if we put a microball on the water surface, we change a molecular field in the vicinity of the ball border and, consequently, the surface tension. Let us discuss here how the presence of the microballs can influence the tension measurements by the Wilhelmy plate [7, 8].

Figure 4 shows the floating microballs and the Wilhelmy plate touching the water surface. The surface tension is measured by a balance as a force F_σ, acting on the Wilhelmy plate. For pure water the force is:

$$F_\sigma = 2\sigma l \tag{2}$$

where σ is the surface tension of pure water and l is the width of the plate. As we discussed, each microball changes the surface tension in the vicinity of its border. Thus, each microball close to the Wilhelmy plate decreases the pulling force of the plate. We can describe this decrease in terms of screening of the plate border from the pure water and the effective decrease of its width.

Let us associate the screening length coming from one microball as l_s. The l_s depends somehow on the distance from a microball to the Wilhelmy plate and, consequently, on the surface density of the microballs. If the surface density of the microballs is n then the quantity of the microballs per width

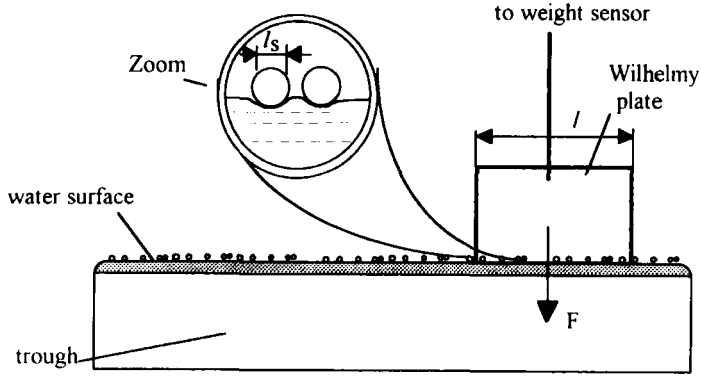

FIGURE 4 Floating microballs and the Wilhelmy plate touching the water surface.

of the Wilhelmy plate is:

$$N = I\sqrt{n} \tag{3}$$

The total screening length will be $NI_s(n)$. Thus, the measured pulling force depends on the microball surface density as follows:

$$F = 2\sigma[I - NI_s(n)] \equiv 2\sigma I[1 - I_s(n)\sqrt{n}] \tag{4}$$

Traditionally, Langmuir–Blodgett equipment is established to measure the difference between the surface tension of the water with a monolayer and that of a pure water surface. In the case of a surfactant monolayer, this difference is attributed to the lateral pressure of a monolayer and called the surface pressure π. In the case of microballs, according to Eqs. (2) and (4), the surface "pressure" of microballs (as the difference, not the real lateral pressure) measured by the Wilhelmy method depends on the surface density of the microballs as follows:

$$\pi \propto I_s(n)\sqrt{n} \tag{5}$$

We underline that I_s itself is a function of the surface density. We can assume an exponential dependence of the screening length *versus* the distance between a microball border and the Wilhelmy plate. At given surface density the average distance between the surface of the closest microballs and the Wilhelmy plate is:

$$t^* = \frac{1}{2\sqrt{n}} - r \tag{6}$$

Thus, the screening length can be expressed as:

$$I_s = \mathrm{e}^{-(1/2\xi\sqrt{n})+(r/\xi)} \tag{7}$$

where ξ is a characteristic screening length. Taking into account that the surface density can be expressed in terms of the average area per one microball as $n = 1/A$, we write the dependence of the surface pressure as follows:

$$\pi = \frac{1}{\sqrt{A}} f_o \mathrm{e}^{-(\sqrt{A}/2\xi)+(r/\xi)} \tag{8}$$

where f_o characterises the maximal pushing force coming from one microball.

The experimental dependence of the surface pressure *versus* the average area occupied by a microball is shown in Figure 5. The area A is shown in arbitrary units. It is due to the quantity of the material, which remains on the water surface, and can not be defined as a quantity of the material we put on. This is the result of involving some microballs into the water bulk as has been discussed above. Nevertheless, abscissa data can be calibrated using direct observation by microscope. We observed the densest microball monolayer at the surface pressure of 28 mN/m, when the area per one microball was of about $16\ 10^{-12}\,m^2$.

Figure 6 shows experimental and theoretical π-A dependences in a proper coordinate frame, wherein the dependence expressed by Eq. (8) should be linear (the abscissa data are shown as $A^{1/2}$, while ordinate data are $-\ln(\pi A^{1/2}/f_o)$. One can see that the experimental data do demonstrate the linear dependence. The best coincidence of the experimental data with that predicted by Eq. (8) are at

$$f_o = 1.2\,10^{-4}\,\text{mN and } \xi = 1.4\mu\text{m}.$$

Equation (8) describes the surface pressure dependence assuming that no other impurities are introduced onto the surface together with the microballs. In fact, there are two sources of the impurities. The first one is the alcohol itself. The second one is associated with the microballs. We used

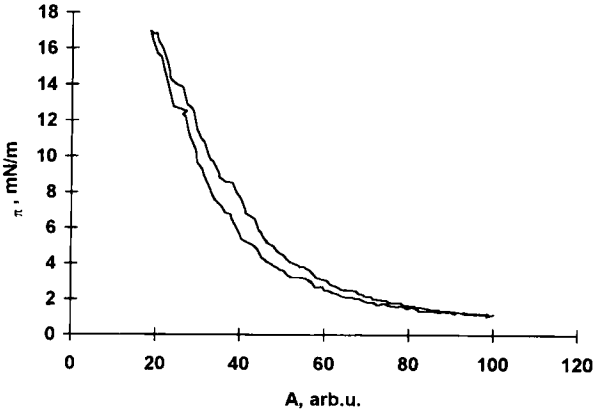

FIGURE 5 Experimental dependence of the surface pressure π *versus* the average area A occupied by a microball.

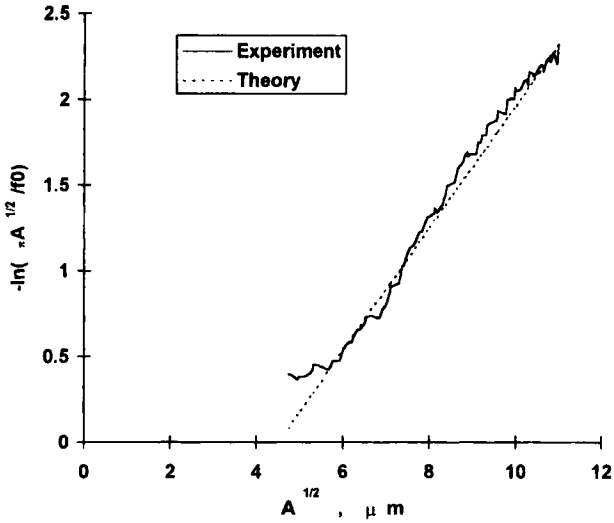

FIGURE 6 Comparison of experimental and theoretical (Eq. (8)) dependences of the surface pressure *versus* the average area occupied by a microball.

commercially available polymer microballs (liquid crystal display spacers, $d = 4.5\,\mu m$). Experimentally, we found that both the surface of the microballs and alcohol were not perfectly pure. It was checked by the registration of the surface tension changes under conditions when no microballs were allowed to be in the vicinity of the Wilhelmy plate during the mixture spreading. Proper purification of both microballs and ethanol can result in a significant decrease of the defects, which arise under formation of a dense microball monolayer.

Despite the MBM being homogeneous on a macroscopic scale (0.1 – $100\,cm^2$), one can see two types of defects (Fig. 3c). The first type is attributed to the holes in a dense monolayer where the hexagonal packing is missing. By analogy with the natural crystals, this kind of defect can be attributed to dislocations. They are about one microball in size and fill up about 0.5% of the total area. The second type, which we call double-layer defects, is related to the local collapse of a monolayer and the formation of a bilayer (in Fig. 3c they look like black spots). The reasons for the defect formation are suggested for further investigations. At this stage one can assume that both surface impurities and the domain texture of the monolayer play an important role in the formation of the defects. Anyway, even under the rather standard conditions we used, when no special precautions were taken, the quantity of the defects was unexpectedly small.

2.3. Transfer of Microball Monolayers onto a Solid Substrate

In principle, there is no limitation with respect to the material of the substrate. A most important point is that the surface of the substrates must be clean and free of macroscopic defects. Otherwise, they can create a local lateral pressure and destroy the homogeneity of the MBM on the water surface. We used the standard commercial available ITO glasses of $20 \times 20\,mm^2$ in size. We cleaned them of dust by air stream with further washing in purified alcohol. Experimentally, we found that no glue sublayer was necessary to allow further transfer of MBM from a water surface to the glass substrate. It reveals that Van der Waals forces are strong enough to allow the MBM transfer onto the substrate. Obviously, the mechanical strength properties of the MBM are not so high.

We did succeed in transferring the MBM monolayer from the water surface onto the substrate by the Langmuir–Shaefer (LS) or horizontal lift method [7, 8]. The microball film on the substrate was found to be non-homogeneous (Fig. 7). The transfer procedure results in a decrease of the density of the microballs in some regions of the substrate and a proper increase in the others, leading to the formation of double-layer defects.

Much better results were obtained using the Langmuir–Blodgett method. Figure 8 demonstrates the procedure used for the transfer of the MBM by the LB method. We have used the unique property of our LB equipment allowing *Z*-type transfer. The trajectory of the substrate is as follows. From the initial state (*a*-position in the figure) it rotates in a counter-clockwise

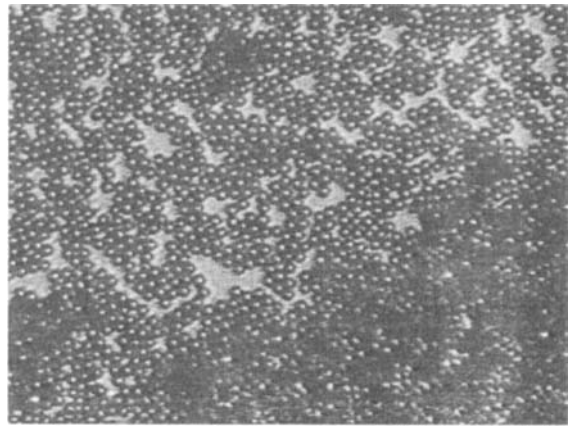

FIGURE 7 Photograph of microball monolayer transferred onto the substrate by the LS method magnified in 200 times.

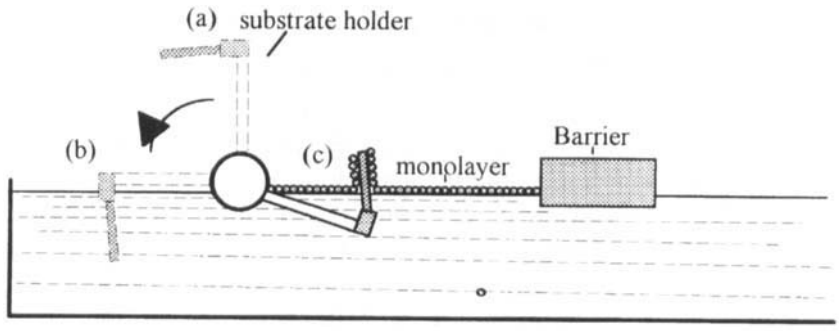

FIGURE 8 Procedure used to transfer the microball monolayer from the water surface onto the substrate.

direction. First, the substrate crosses the buffer zone with the pure water surface (*b*-position in the figure); then, while elevating the substrate in the working region (*c*-position), the compressed monolayer transfers onto the substrate. The important point is to support the surface pressure at a given value during the procedure. The transfer procedure is automated using the computer and specially designed software. Figure 9 shows the photograph of MBM prepared at the surface pressure of 28 mN/m. The homogeneity and the density of the defects in this case are much better than those of the LS method. Actually, the quantity of the defects is close to that on the water surface.

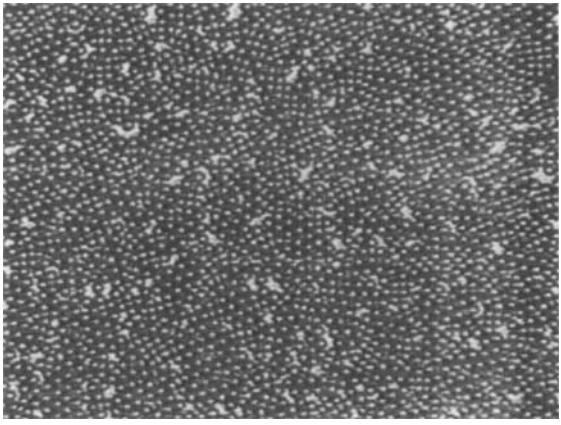

FIGURE 9 Photograph of microball monolayer transferred onto the substrate by the Langmuir–Blodgett method magnified in 200 times.

3. MBM PROPERTIES

3.1. Optical Properties

We consider the optical study of the phase-grating produced in a well-ordered monolayer of 4.5 μm polymer microballs on a solid substrate using the diffraction pattern of a parallel laser beam, incident normally on the monolayer.

A polydomain structure of polymer-indentical microballs on a solid substrate has been produced by the LB technique, Figure 9. A narrow parallel laser beam (5mW He – Ne, $\lambda = 0.63$ nm) is incident perpendicular to the glass covered with polymer microballs. The hexagonal packing of solid balls in each domain gives rise to the regular diffraction pattern of a laser beam. We observe, on a screen normal to the beam, a series of diffraction rings, imaging the randomly distributed regular gratings (the analog of X-ray diffraction in powder). The diffraction angle ψ is related quite generally to the period of the diffraction structure D by:

$$\sin \psi = n\lambda/D, \tag{9}$$

where n is the order of the ring, and λ is the wave length. The intense series corresponds to a diameter of the microballs (4.39 μm). It is worthy to notice that, in the case of randomly distributed microballs of the same dimension, the first diffraction minimum is defined as:

$$\psi = 0.61\,\lambda/D \tag{10}$$

Figure 9 clearly demonstrates that the monolayer of the microballs also gives rise to the formation of the focal centres of period D, formed due to the refraction of the laser beam on the surfaces of the microballs. This fact significantly complicates the rigorous theoretical consideration of the phase-amplitude grating diffraction. In our consideration, we will examine only the phase-grating mechanism. It should be noted that this approach was good enough for the case of a related optical problem: electrohydrodynamical periodic instability in nematic liquid crystals (Williams low frequency domains) [9].

If a plane wave of unit amplitude is incident on a grating, the optical distribution just behind the grating may be calculated as a function $u(x)$. The diffraction pattern of the grating at infinite distance is the Fourier transform of $u(x)$. An equivalent approach is to calculate $u(x)$ as a

superposition of plane waves. Each spot of the diffraction pattern can be shown to be the Fourier transform of one of these plane waves. The main point of the diffraction calculus is then the determination of $u(x)$ generally known as "amplitude transmittance of the grating". In the case of normal incidence following [10], we express $u(x)$ as:

$$u(x) = u_o \exp\left[ik \int_0^D n_{\text{eff}}(z)dz\right] \tag{11}$$

where $k = 2\pi/\lambda$, and λ is the incident wavelength. For the phase-grating consideration the experimental situations shown in Figure 10 (a and b) are indentical and due to the symmetry we get:

$$u(x) = u_o \exp\left[2ik \int_0^{D/2} n_{\text{eff}}(z)dz\right] \tag{12}$$

Consequently, it is enough to analyse the diffraction pattern from the semispheres shown in Figure 10b instead of one from the microballs. The standard procedure is to approximate the surface of sphere S by harmonic function:

$$S \cong D/4\left(1 - \cos\frac{2\pi x}{D}\cos\frac{2\pi y}{D}\right) \tag{13}$$

Thus, the refractive index spatial distribution is defined as:

$$\begin{aligned} z \leq z_o, \ldots n_{\text{eff}} &= n_{\text{ball}} \\ z > z_o, \ldots n_{\text{eff}} &= 1 \end{aligned} \tag{14}$$

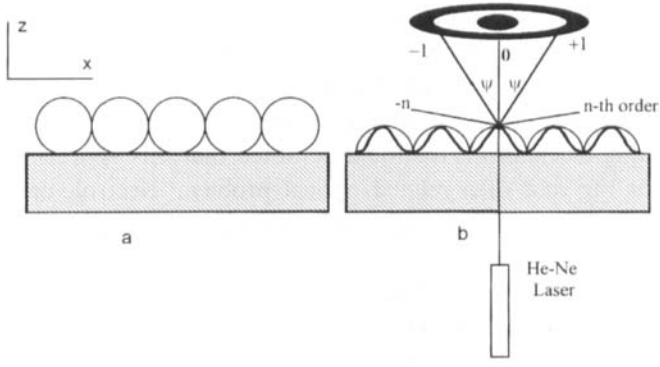

FIGURE 10 Geometry of the diffraction experiment.

where n_{ball} is the refractive index of the polymer microball and z_o is defined as:

$$z_o = D/4[1 - \cos(2\pi x/D)\cos(2\pi y/D)] \tag{15}$$

Each domain with regular hexagonal packing will form a diffraction spot at the diffraction ring in accordance with the orientation of randomly distributed axes of hexagonal lattices. For $y = 0$ one gets:

$$u(x) = u_o \exp\{2ik[(D/4(n_{\text{ball}} + 1) + (n_{\text{ball}} - 1)\cos 2\pi x/D)]\} \tag{16}$$

or

$$u(x) = u_o \exp\left[\frac{ikD}{2}(n_{\text{ball}} + 1)\right] \exp\left[\frac{ikD(n_{\text{ball}} - 1)}{2}\cos\frac{2\pi x}{D}\right] \tag{17}$$

(In essence, we approximate the randomly distributed scattering domains with hexagonal packing of spherical balls by cylindrical lenses with random distribution of their axes).

The diffraction pattern is given by Fourier transform of $u(x)$ and can be calculated using the following formula:

$$\exp[iq\cos\alpha] = \sum_{n=-\infty}^{n=+\infty} \exp[in(\alpha + \pi/2)J_n(q), \tag{18}$$

where $J_n(q)$ is the n-th Bessel function. One should note that, if the left side of this expression is considered as a complex-shaped wave, the right side gives its decomposition into an infinite superposition of plane waves. The n-th plane wave of that decomposition gives the n-th spot of the diffraction pattern whose intensity is:

$$I_n = \|A_n\|^2 = \|u_o\|^2 J_n^2(q), \tag{19}$$

where for our special case $q = (\pi D/\lambda)(n_{\text{ball}} - 1)$

The diffraction patterns from frosted glass and monolayers of microballs are shown in Figures 11 and 12–14, respectively. The diffraction pattern from frosted glass looks like the diffusion spot and corresponds to the

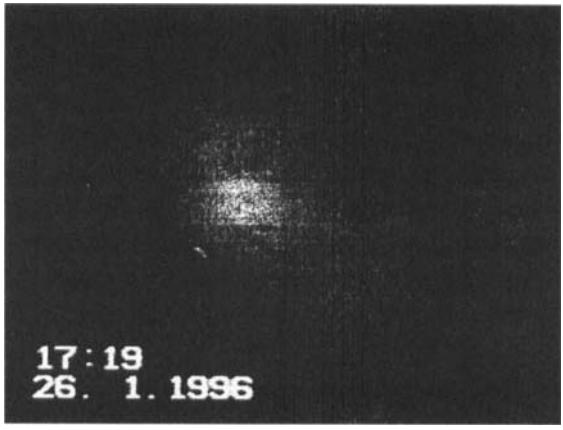

FIGURE 11 Diffraction pattern from frosted glass.

diffraction from randomly distributed regions with the randomly distributed dimensions of scattering centres.

Figure 12 shows the diffraction pattern of a monolayer of randomly distributed identical polymer microballs formed in LB films of low quality. In this case, the direction on the 1-st diffraction maximum is represented by Eq. (10). The diffraction pattern from well-ordered randomly distributed regions with hexagonal packing of polymer microballs is shown in Figure 13. The average diameter of the microball $d = 4.39\ \mu m$ was calculated using Eq. (9).

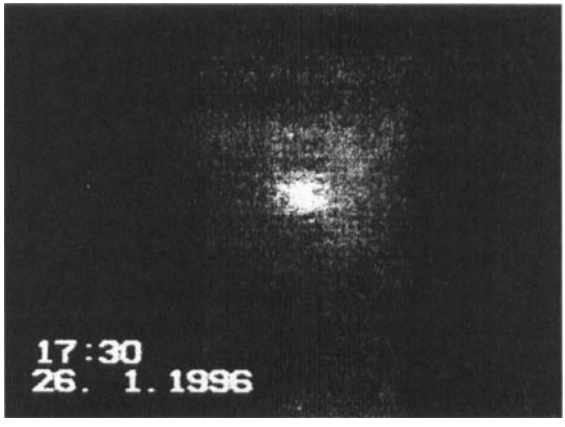

FIGURE 12 Diffraction pattern from the monolayer of microballs (low-quality packing).

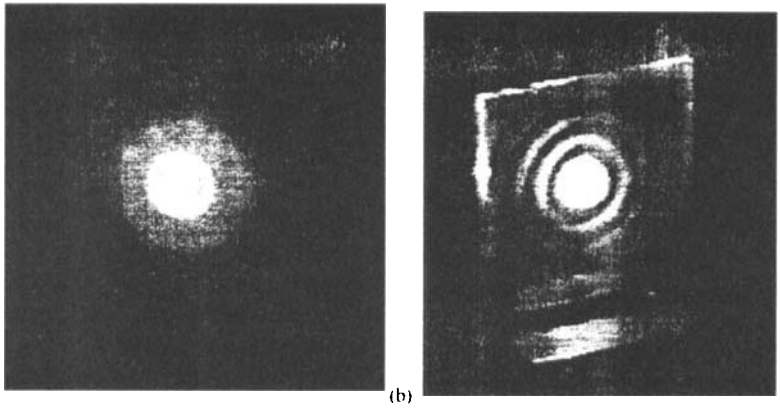

FIGURE 13 Diffraction pattern from the monolayer of microballs (good quality). a) on the glass surface; b) on the screen.

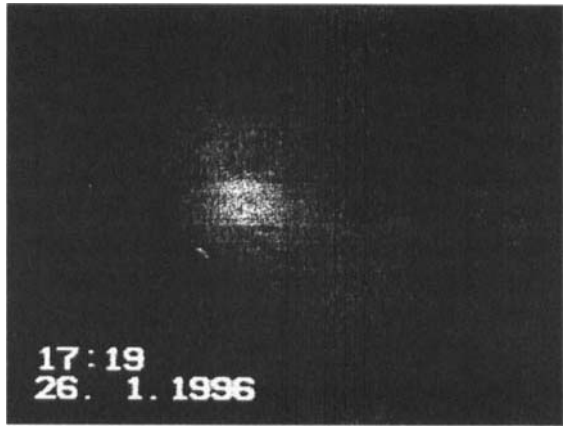

FIGURE 14 Laue diagram from well-ordered cylindrical holes formed into the glass substrate.

As an illustration of the perfect arrangement of scatering objects, Figure 14 shows a classical Laue diagram from well-ordered cylindrical holes formed into the glass substrate. To check the validity of the model of the phase diffraction grating the ratio between the intensities of the diffraction rings and intensity of the incident laser beam have been measured. For the zero-th order spot we measured I_0/I_{total} to be equal 0.032 and $q = 11$ that corresponds to $n_{\text{ball}} = 1.502$ (I_0 is the transmitted light intensity in the zero-maxima and I_{total} is the laser beam intensity).

In conclusion, in the framework of the Born approximation, we have analysed the diffraction pattern from polymer microballs forming the

monolayer on the glass. The average diameter and refractive index of the microballs have been measured. The average diameter of the microballs measured by the diffraction technique (4.39 μm) was very close to the diameter of the microballs measured by microscope (4.5 μm). The calculated value of the polymer microball refractive index ($n_{ball} = 1.502$) has a reasonable value which is typical for polymer materials.

3.2. Nematic Cell with MBM

Figure 15 demonstrates the diffraction pattern from the monolayer of the polymer microballs covered with a layer of homeotropically oriented nematic liquid crystal:

4-*n*-pentyl-4'-cyanobiphenyl (their total thickness is 10 μm). The matching of refractive indices of polymer microballs and nematic liquid crystals gives rise to the redistribution of the intensities of the diffraction rings with respect to a monolayer in contact with air and increases the transmitted light intensity in the 1-st diffraction maxima. The diffraction pattern was stable at least during 3 months, which proves the high adhesion properties of the microball monolayer to the glass substrate.

The most important point is that the diffraction pattern of the nematic cell can be controlled by an external electric field. We assume that by choosing the proper nematic liquid crystals (NLCs), one can achieve significant changes in the optical properties of nematic cells. The latter can be very important for liquid crystal display applications and it is demonstrated in

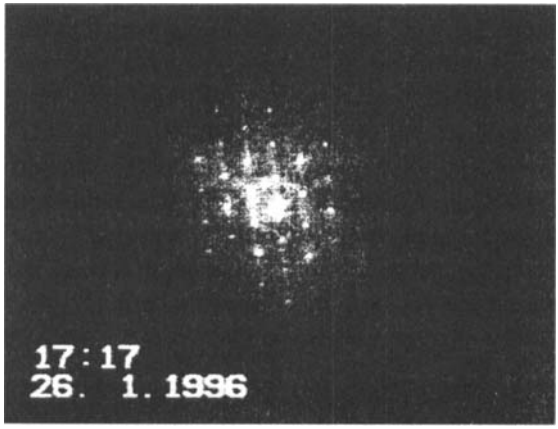

FIGURE 15 Diffraction pattern from the monolayer of polymer microballs covered with a layer of homeotropically oriented nematic liquid crystal: 4-*n*-pentyl-4'-cyanobiphenyl.

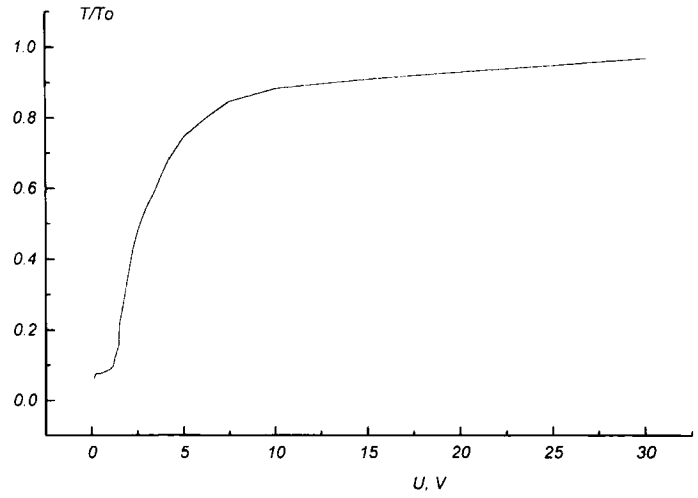

FIGURE 16 Transmission *versus* applied voltage dependence of the nematic cell having no polarizers and comprising the polymer microball monolayer, the layer of homeotropically oriented 4-*n*-pentyl-4'-cyanobiphenyl sandwiched between two ITO glass substrates.

Figure 16 by the transmission *versus* applied voltage curve of the nematic cell comprising the polymer microball monolayer, the layer of homeotropically oriented 4-*n*-pentyl-4'-cyanobiphenyl (their total thickness is 10 μm) sandwiched between two ITO glass substrates, having no polarizers and utilizing the effect of light scattering at boundary layers.

4. CONCLUSION

We developed the procedure of spreading polymer microballs onto the water surface, observed and investigated the formation of the dense polymer microball monolayer on the water surface using a specially designed set-up.

We found that the Langmuir–Blodgett method of transferring the polymer microball monolayers from the water surface onto ITO glass plates leads to more homogeneous film in comparison with the Langmuir–Shaefer method.

The prepared films of polymer microballs have been investigated by the optical microscopy and diffraction methods. All the results demonstrate that the microballs are well-packed in the monolayer. The preliminary investigations of the optical and electro-optical properties of nematic liquid crystal cells prepared with the microball monolayer show that NLC

influences the optical diffraction from the microball monolayer. This influence can be controlled by switching NLC molecules with the help of an external electric field, and it was demonstrated experimentally showing that a novel polymer–liquid crystal system is suitable for liquid crystal display applications.

References

[1] W. J. Doane, *Liquid Crystals, Applications and Uses*, Edited by B. Bahadur (World Scientific, Singapore, 1990), Chapter 14, pp. 361–395.
[2] J. L. Fergason, US Patent 4435047, 1984.
[3] P. S. Drzaic, *Liquid Crystal Dispersions* (World Scientific, Singapore, 1995).
[4] I. Langmuir, *J. Chem. Phys.*, **1**, 756 (1933).
[5] K. B. Blodgett, *J. Am. Chem. Soc.*, **57**, 1007 (1935).
[6] S. G. Yudin, S. P. Palto, V. A. Khavrichev, S. V. Mironenko and M. I. Barnik, *Thin Solid Films*, **210/211**, 46 (1992).
[7] G. L. Gaines, *Insoluble Monolayers at Liquid–Gas Interface* (Interscience, New York, 1966).
[8] H. Kuhn, D. Mobius and H. Bucher, *Techniques of Chemistry*, Edited by A. Weissberger and B. W. Rositer (Wiley, New York, 1973).
[9] T. O. Carrol, *J. Appl. Phys.*, **43**, 767 (1972).
[10] H. Kogelnik and T. Josnowski, *Bell. Syst. Tech. J.*, **49**, 1602 (1970).